EFFECT OF ABSORBER PLATE HEIGHT ON THE PERFORMANCE OF SOLAR CHIMNEY UTILIZED WITH POROUS ABSORBER AND INTEGRATED WITH AN INSULATED ROOM

by

Suhaib J. SHBAILAT[a*] and Mohammed A. NIMA[b]

[a]Department of Biomedical Engineering, Al-Esraa University College, Baghdad, Iraq
[b]Department of Mechanical Engineering, College of Engineering, University of Baghdad, Baghdad, Iraq

Original scientific paper
https://doi.org/10.2298/TSCI211008117S

An experimental study has been carried out for testing the thermal performance and the thermal behavior enhancement of solar chimneys that can be achieved by adding metal foam. The solar chimney with test room system was located in Baghdad, Iraq, at latitude 33.3° N, longitude 44.4° E. In the experimental part of this study, outdoor tests were conducted from May to July, 202). On clear days, the tests were conducted from 9:00 a. m. to 4:00 p. m. The experimental side will compare the performance of two types of copper metal foam, 10 PPI and 40 PPI, (pores per inch) heat absorber plates at three different heights, 5 cm, 15 cm, and 25 cm. The results showed that the metal foam reduced the average temperature of the absorber plate. The highest temperature reduction was achieved with, 10 PPI and 40 PPI, absorber plates, 13.5 °C and 8.3 °C, respectively, at (H = 5 cm) and 60°. The maximum increase in air-flow velocity at the solar chimney with, 10 PPI and 40 PPI, absorber plates is, 43.7% and 25%, respectively, at (H = 5 cm). The absorber plate heights decrease the air velocity at the solar chimney. With metal foam as an absorber plate, 10 PPI and 40 PPI, the chimney's thermal efficiency is increased. At the absorber plate's height, the solar chimney's maximum thermal efficiency was 49%, 66.2%, and 72.1% (5 cm). At the height of the absorber plate, the maximum air change per hour was 18.8, 24.4, and 27.21 (5 cm).

Keywords: *solar chimney, low-energy room, ventilation, metal foam, porous absorber*

Introduction

Energy is the most significant factor influencing human life because it is required for the performance of any type of work in any sector. Consequently, the acquisition of energy is the most interesting object that occupies the minds of the people in order to continue their lives, and on the other hand, energy resources are limited in terms of quantity and location. The rapid and substantial depletion of fossil fuels in recent decades has led to the need for alternative energy sources. These sources should be renewable and sustainable on one hand,

*Corresponding author, e-mail: suhaib@esraa.edu.iq

friendly and non-polluting the environment on the other hand. Ventilation is the process of supplying and removing air from space using natural or mechanical means, depending on the environment. When proper ventilation procedures are followed, the quality of the indoor air can be significantly improved. In these procedures, some of the polluted air is removed from the environment and the remaining pollutants are diluted with acceptable outside air. It is a combination of the air brought in from the outside and any recirculated air that has been treated to serve as ventilation air [1]. Two factors contribute to natural ventilation: aeromotive or wind driving force and buoyancy driving force (stack effect) caused by the temperature difference between indoor and outdoor air temperatures. The buoyancy force is quite low, while the wind force is greater. There are two basic types of ventilation. Wind-driven ventilation relies on wind to supply ventilation while stack ventilation has several benefits. The efficient design for natural ventilation of building must be both types of ventilation. The passive cooling strategy is the use of natural ventilation, which can be divided into three basic strategies, one side ventilation, cross-ventilation, and buoyancy-driven ventilation [2]. The buoyancy-driven or stack ventilation is generally more predictable and more reliable than others. This is because stack ventilation is not dependent on wind speed or wind direction. Ventilation is one of the significant options for supplying buildings with thermal satisfaction. The increased realization of the energy utilize impacts on environment and cost, utilization of natural-ventilation has increasingly become a desirable technique for lowering energy utilize, price and for producing acceptable interior environmental condition and keeping a healthy, relaxation, and constructive interior climate instead of the more common method of mechanical ventilation usage [3]. Thermal buoyancy is also referred to as the stack effect or the chimney effect in some instances. It will be necessary to pull air into and out of a building through special ventilation openings because of the difference in densities, which will result in pressure differences being created [4]. The stack effect is caused by the temperature difference between the two adjoining volumes of air. Due to its lower density and greater buoyancy, the warmer air will rise above the cold air, resulting in an upward air stream. An example of the forced stack effect in a building is found in a traditional fireplace. When it comes to bathrooms and other spaces that do not have direct access to the outdoors, passive stack ventilators are a standard feature. During hot, still days, natural ventilation in buildings is primarily dependent on wind pressure difference, however, the stack effect can augment this type of ventilation and partially restore air-flow rates. In some cases, stack ventilation can be implemented in a way that does not rely solely on wind direction to provide air-flow in a building. In this regard, it has the potential to improve air quality in some polluted environments, such as urban areas.

A solar chimney, often mentioned as an updraft stack, is a technique of enhancement the natural ventilation of a building by heating air convected by passive solar energy. The efficiency of air ventilation and thermal comfort is so important in the hot climate. Solar chimneys are more appealing in applications where temperatures must be kept low and controlled. When it comes to ventilation, natural methods of conditioning buildings are employed, whereas solar chimneys may contribute to reducing the building's energy consumption by reducing the amount of energy required [5]. Due to the heating effect of solar radiation on the air within the chimney, buoyancy forces are created, which cause the air to rise and exit the chimney. In accordance with mass balance, the air exhausted from the chimney induces fresh outdoor air into the building through openings such as doors and windows, thereby providing ventilation for the structure. Increases in the intensity of solar irradiance cause an increase in the temperature, which causes a decrease in the density of air, which causes the air to rise and draw air from the surrounding environment, thus ventilating the space. The solar chimney conventional formations can be a simple duct, typically rectangular, combined to the wall, and roof level solar chimney at the upper or as-part of a solar collector. It is possible to observe the operation of solar chimneys for the purpose of naturally ventilating buildings in ancient buildings, which were supposedly named in Italy *Scirocco rooms* in the 1^{6th} century. The solar chimneys were used in conjunction with underground passageways and water characteristics to improve cooling and ventilation in these buildings, respectively [6]. Because of the lower value of the heat transfer coefficient, the efficiency of an air solar chimney is typically low. To achieve this, a layer of artificial roughness is applied to the upper side of the absorber plate, causing turbulence to flow through it and increasing the value of the heat transfer coefficient [7]. The main problems of the solar chimney are a low value of heat transfer coefficient and thermal capacity of air, the reason for these problems to the physical properties of air. Also, the heat losses from the solar chimney are high about 55% from the incident solar radiation, which reduces the performance of the solar chimney [8]. Highly effectual techniques have been utilized in the preceding researches for thermal-performance improvement that includes the procedures of decreasing the losses of heat in the solar chimney. One of the methods includes using PCM to increase the ventilate time or using fins to enhance the heat transfer. Also, the insertion of porous media in the flow passage of the solar chimney as an absorber plate is a passive method that gives a high heat transfer rate.

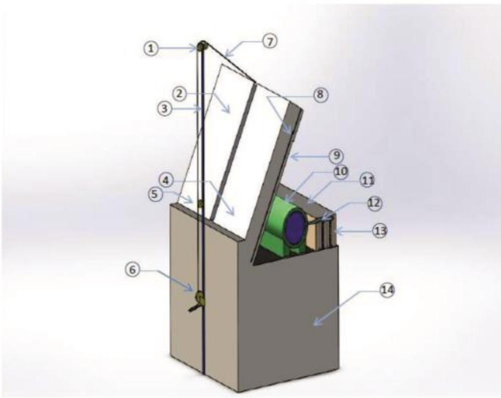

Figure 1. The 3-D schematic diagram for the physical domain; *1 – pulley, 2 – acrylic cover, 3 – lifting stand, 4 – metal foam solar chimney, 5 – flat plate solar chimney, 6 – winch, 7 – steel wire, 8 – absorber foam, 9 – plywood panel, 10 – tank of water, 11 – wind protect, 12 – pipe, 13 – wet pad, and 14 – test room*

The objective of the present work is to investigate the solar chimney performance numerically and experimentally utilized flat plate and copper foam chimney absorber plate integrating with insulated test room, fig. 1. The effect of metal foam absorber plate on the performance of the solar chimney will be studied and presented in this work. Figure 1 shows a physical geometry of the system used in this work.

Metal foam as a heat sink in solar chimney

Metal foam is typically low density porous media with novel structural and thermal properties. Metal foam is presently the most popular heat sinks utilized material. It has comparatively high heat conduction that, is light, is relatively low price, and is resistant to corrosion. Several mechanisms contribute to enhancements of heat transfer related to the utilize of metal foams, involving interfacing between a through-moving fluid and the solid-foam material, where the porous matrix has a larger influence on dissipating the heat from the hot components and then exchanging this heat with the flowing fluid. The second important factor in heat sink performance is surface area per unit volume, which governs heat dissipation through convective heat transfer [9]. Metal foams define as porous materials sort with special characteristics that are utilized in applications of heat transfer with several structures. Metal foams are invented in the 20th century, having many benefits of ultra-light, uniform pore size, high porosity ($\varepsilon > 0.8$). In the proceeding years, the attention was directed toward heat transfer and fluid flow enchantments in metallic foams, due to the high thermal conductivity ratio between the solid matrix and the fluid passes through it, large surface area to volume ratio of the heat transfer process (500~10000 m^2/m^3), and increasing the flow mixing capability as a result of the tortuous paths inside the porous matrix [10].

Metallic foams are known to have many mechanical properties including:

- Low weight.
- Giving exceptional heat transferability.
- Resistance to thermal wear, high temperature, humidity, and shock.
- Good influence energy absorption.
- Excellent mixing of fluid due to tortuous flow path.
- Excellent noise reduction.

Metal foam can be used as a disturbance or guider to the flowing fluid (besides its thermal properties and heat transfer functions) when it is set inside the solar chimney with a special arrangement. Metal foam can be cut easily, formed with different shapes as shown in fig. 2, and set inside the solar chimney at a different height. The advantage of disturbing the fluid is to distort the flow structure and diffuse the heat in all the domains. Open-cell metal foam structure with some properties like low pore density and low permeability can be considered as a good director and blowing to the fluid-flows inside the solar chimney [10].

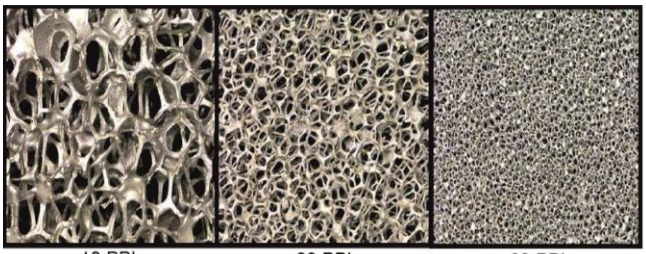

Figure 2. Types of metal foam

Literature Survey

Shao and Riffat [11] designed natural ventilation system with a passive stack. The system was designed without heat recovery because the heat recovery caused pressure drop across the conventional heat exchanger (HE), and that leads to failure for ventilation systems. So individual heat pipe, with high thermal conductance and low pressure drops than from the conventional HE, was located in ventilation stacks. Results from experimental work showed that, for a heat recovery efficiency of 50% and stack flow speed of 0.5 m/s, the pressure loss across an inclined heat pipe was about 1 Pa. In [12] the theory and practice of solar chimneys to induce natural ventilation and the impact of the openings' doors, windows, and an inlet of solar chimneys on ventilation were both investigated and experimentally examined. The room was about 25 m^3 in volume, and the study used it as a single-room schoolhouse. Each of the chimneys had three different configurations of solar chimneys, and the total surface area was 2 m^2 for each. When the solar chimney ventilation system was in use, the temperature in the building or test room was near the temperature of the surrounding air. Reducing the building's heat gain is a good indication of good ability in the solar chimney. The results vary from about 8-15 ACH in that particular study. Additionally, the data showed that opening windows and doors results in less energy efficient than using solar chimneys, resulting in higher temperatures between buildings and the surrounding environment. Raman *et al*. [13] studied experimentally the natural ventilation system which gives cooling in hot weather or heating in cold weather dependent on the season of the year. Some of the famous systems which are appropriate for combined weather in this category are barra-costantini system, the silvestrini bell, the earth-air tunnel, and the sky-therm. This paper was developed and described the natural ventilation system, which can produce thermal comfort through the year in combined weathers. Northern and central India which contains large areas has combined weather as hot-humid, hot-dry, and weather conditions. Model 1 including two sets of solar chimneys was improved and observed for its performance in the first stage for 1 year. In Model 2 the sack-cloth cooling and Trombe wall models were integrated for making it more efficient and also to give it a more appealing look. Kotani *et al*. [14] developed the solar chimneys with built-in latent heat storage material to induce natural ventilation in the evening and night. The simulated and experimental results showed that the integration of PCM storage inside the solar chimneys was effective, and it can supply a nearly constant air-flow rate of 155 m^3/h, with 0.2 m air gap, 45° at inclination angle, in evening and night, in condition when the PCM completely melting during the day. The prototype solar chimney was capable to provide nearly 200 m^3/h with a 0.2 m air gap, and 45° of inclination angle in the daytime interval from (6:00 a. m. to 5:00 p. m.). Also, the results referred to that the PCM did not melt with a solar radiation value less than 325 W/m^2. Lipska [15] present the problems and errors associated with CFD-based air distribution predictions. The possible sources of error were found as well as program options and experimental identification of the predicted flows to see if they could be eliminated or reduced. Ceiling square cone diffusers were combined with displacement ventilation systems, as well as laminar diffusers. 96250, 376272, respectively, (346104). To perform numerical calculations, we used FLUENT 6.1. In order to find out if the air-flow pattern and contaminant propagation were correct, we measured how well the predictions matched with visual observations of the actual flow. The predicted and measured parameter profiles were compared. By using default settings and grid discretization of the CFD code, the results of predicting the parameters of air and gaseous contaminants in a ventilated room failed to agree with the measurement results for both mixing and displacement configurations. The flow and previous experiences in numerical modeling of the buoyant plume in simple ventilated rooms were used to identify appropriate options. Leticia *et al*. [16] showed that the possibility to optimize the solar irradiation on the absorber plate, and ensure a considerable stack height by using solar chimneys extension, with a minimum height of solar chimneys. Simulation results were compared with experimental test results, that testing the air-flow enhancement, and referred to the ability to use a normal ventilation strategy in Brazilian at low latitude locations. A mass-flow rate equation was used to calculate the discharge coefficient, Cd, where, the resistance for the air-flow through the solar chimney channel is included. Inlet and outlet openings input wind pressure coefficients were found in wind tunnels. Amori and Saif [17] presented a numerical and experimental study for solar chimneys that was designed, manufactured, and tested with different air entrance positions, to the solar chimneys. A bottom entrance, side, and both entrances together were tested. The effect of PCM (paraffin wax) employed in the solar chimney was also studied. The FVM was used to calculate the thermal performance of solar chimneys under transient conditions using a mathematical model of CFD. Several different parameters were studied, such as solar radiation and inclination angle. Results showed that a higher performance was obtained when the air entrance from the side of solar chimneys. While adding the PCM to the solar chimneys like a thermal energy storage chimney, the ventilation period time was extended, so, the effect of solar chimneys on ventilation was appeared not in the daytime, but also in the nighttime. In [18], The design and analysis of a solar system for climates with mild or warm temperatures are discussed in this study.

The well-known software FLUENT is used to demonstrate the structures of these systems and finally compare the results with numerous instances already researched in order to improve the performance of the solar chimney system. The design of the solar chimney system takes into account extremely efficient subsystem components. In order to better understand how solar chimney systems create cooling, and to increase the efficiency of such systems for use in present and future home structures, the project aims to gather data. Touma *et al*. [19] proposed a hybrid system used on the surface of glaze for reduction the space cooling load and radiation asymmetry which was studied to investigate the performance of this system. The inside air entered the test room is due to the natural buoyancy flow of the solar chimney and evaporative cooler which is the suggested system. An analytical heat and mass transport model merging the solar chimney, glazing section, office space, and an evaporative cooler is improved for studying the performance of this system in hot and dry weather. The improved model was confirmed during experimental proceed in a dual weather room for known solar radiation, humidity, and ambient temperature conditions. Zha *et al*. [20] evaluated ventilation performance in the summer months, for three solar thermosyphon configurations with high thermal inertia, with and without nighttime natural ventilation. In this study, the configurations and their orientations were investigated to discover which worked best at night-time ventilation. Air-flow rate: 1887.6~1870.6 m^3/h in a 6.2 m solar chimney with a 2.8 m width and a 0.35 m air gap. Three distinct designs for solar chimneys were constructed and put through their paces. Through the transitions between April and October, Shanghai's solar chimney can save energy with an energy-saving rate of 14.5%. The results from the simulation were compared to those obtained through published research. The findings from the analysis state that the second solar chimneys design with west-facing windows was the most effective. Solar chimneys concrete with 3 m of vertical height, 0.2 m of horizontal gap depth, and 0.1 m of wall thickness exhibited cooling capacity during the night, these properties depended on the position of the solar chimney and the setup of its facing panels. The capacity of the chimney was measured with face-to-face orientation. Sujeeva *et al*. [21] is the first study to combine energy-saving and fire safety considerations while proposing a real-world design for a solar chimney. Once validated, all the typical designing factors on both functions were investigated with a numerical tool. Additionally, data suggest that solar chimney is usable in both capacities, with air change requirements of 7.42 air changes per hour with natural ventilation, and a minimum requirement of 6.52 times more extension of available egress time for occupants in the event of a fire. This cavity gap of 0.2 m to 0.3 m was also reported to no longer be useful for a larger space where the optimum gap of 1.2 m must be considered for both functions. It is proposed that a positive consistency coefficient is a parameter that increases the overall performance, while a negative coefficient compromises overall performance. In [22], an evaporative cooler and two particle sizes, 10 PPI and 40 PPI, metal foam absorber plates in the solar air chimney have been integrated into the test room and solar air chimney to increase heat transfer characteristics and overall performance. A comparison of the metal foam absorber plate's natural convection heat transfer performance at various inclination angles with that of a standard flat absorber plate is made. Three varieties of chimney absorber plates (flat, 10 PPI and 40 PPI) will be tested in Iraqi weather conditions and with four different inclination angles of the metal foam absorber plate during the months of January, May, June, and July in 2021. In terms of various absorber plate heights and inclination angles, the experimental result obtained with a 10 PPI absorber plate is superior to that obtained with a 40 PPI absorber plate. Solar chimneys with different absorber plates, such as 10 PPI or 40 PPI, are utilized in the experiment to compare the data obtained from the two identical solar chimneys. Jing and Liu [23] showed it is common for mountain houses to be constrained by the landscape. In the mountainous region of Taihang, a passive solar building design strategy is proposed that takes advantage of the building's location next to a mountain's shady courtyard to act as a cold source for the surrounding outdoor environment. Passive solar building techniques can be successfully applied to mountain dwellings by this design.

From the previous studies, it is concluded that the passive solar chimney effect can be used in different modes, like heating, cooling, and ventilation. All modes depend on the effect of buoyancy force generated. That force (buoyancy) impacts the quantity of air volume flow rate which is ventilated by the solar chimney and cooled via evaporative cooling, so employing the heat absorber media leading to increase heat transfer and temperature difference which in turn leads to increase buoyancy force. Many experimental studies investigated employing the metal flat plate as heat absorber media but without mentioning whatever about examine the possibility of enhancing the thermal behavior of a solar chimney through adding porous materials. The present work investigates numerically and experimentally the thermal behavior enhancement of solar chimneys that can be achieved by adding metal foam. Others concluded about the previous studies of the modes referring to the effect of general parameters like the solar irradiance, aspect ratio, chimney height, inclination angle of the chimney, chimney face orientation, induced are from the green area, *etc*. all these parameters affected to the volume flow rate of air and its temperature.

Experimental work

The solar chimney with test room system was positioned in Baghdad city, Iraq, where the solar chimney was directed to the south and situated at latitude 33.3° N, longitude 44.4° E. It is designed, manufactured, and tested to study the effect of some parameters that affect the performance of the solar chimney in steady-state conditions. Initial tests have been conducted on the system, during which the positions of the velocity, thermocouples, pressure, and humidity measurements taps have been determined, as well as the evaluation and resolution of rig manufacturing snags. The outdoor tests were carried out side by side during the period from May to June 2021. The experiments were carried out from 9:00 a. m. to 4:00 p. m. for clear days. The experimental side is to test two types of copper metal foam, 10 PPI and 40 PPI, as a heat absorber plate with different inclination angles, θ, (30°, 45°, 60°, and 75°) and compare the performance of the metal foam absorber with that of the conventional flat absorber plate. Figure 3 shows the photographic view of the experimental set-up. This model consists of the evaporative cooler, solar chimney, and test room enclosed in insulation and two types of copper metal foam, 10 PPI and 40 PPI, as a heat absorber plate and without metal foam. The inclination angle for the solar chimney is varied at θ: 30°, 45°, 60°, and 75°.

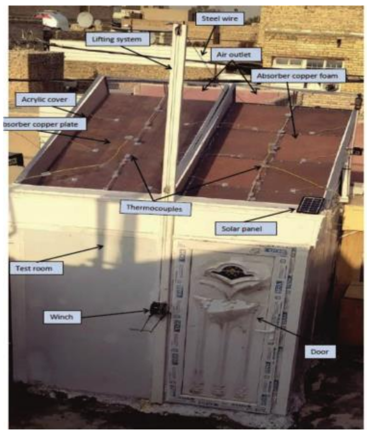

Figure 3. Experimental apparatus

Solar chimney

A vertical chimney is built into the test room so that it can be used for the heating, ventilation, and cooling modes. It is intended, through a connection of a wood box in the wall of the southern room, that makes a chimney that is designed to be conducted to the south. From the outside, the upper side of the solar chimney is covered by a transparent acrylic clear sheet, which covers only half of the chimney. The lower half is connected to the test room via a 2 m long insulating thermal path, where the thermal path has an angle of 30°, 45°, 60°, and 75°. This structure was designed with the dimensions of the collector in mind. They are 2 m long by 1 m in width and air gap of 0.3 m. The absorber side of the solar chimney is under-exposed to the sun's rays (absorber). Rectangular compartments or openings are made in the chimney pipe as the air inlet and the threaded hole as the air outlet. The solar chimney's structure is made up of a 2.5 mm thick iron frame with a surface area of (2 × 1) m^2 and a stud to connect the iron frame at one end. Solar chimney insulated on the sides and bottom of each chimney with plywood and the acrylic layouts is covered at the top of each chimney. To reduce heat loss in the gap, 2 cm thick wood is chosen, and high temperature silicon rubber is used at the wood's corner to prevent any air leaks. The absorber height, *H*, is the height of the absorber sheet, can set it and lifting the absorber sheet by the screw which fixing on an iron frame of the chimney as shown in the fig. 3. Figure 4 illustrates the side-view for this particular test room.

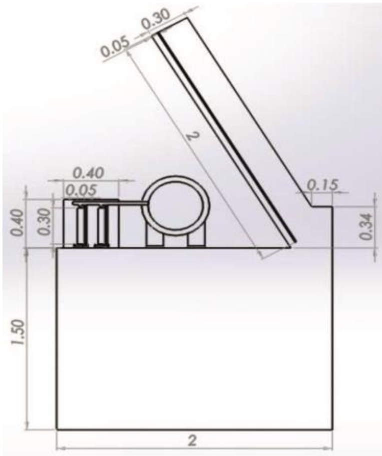

Figure 4. The Side-view for test room

Copper foam sheets absorber

It uses, 10 PPI and 40 PPI, of copper foam sheets on the experimental work. The Chinese (Beihai Composite Materials Co., Ltd) company has shipped some copper foam sheets, size of (50 × 50) cm^2 and thickness of 10 mm. The sheets are sufficient to cover the construction area of 2 m^2 for each type of copper foam absorber. Eight sheets are used for each type, 10 PPI and 40 PPI, of processed absorber sheet. When sheets overlap each other by 1 cm, the contact is optimal. Training and studies at the University of Technology of Iraq is done with a CNC milling machine (vector 610) and a high-speed steel tool (d = 12 mm) [24]. The sheets are also cut with the CNC milling machine to achieve overlapping the sides of the sheets. Thermal conducting adhesive (k = 9 W/mK) is used in the overlapping sections to lower the contact resistance between the metal foam sheets. To fix the sheet metal plates to each other, steel bars (w = 12.5 mm) are used with bolts (d = 5 mm, L = 25 mm) with 10 cm pitch along the overlapped sections to ensure the mounting of these sheets with a strong bonding contact and to convert into one copper metal foam absorber plate. The copper foam plates showed the final form in which its application would be performed as shown in figs. 5 and 6.

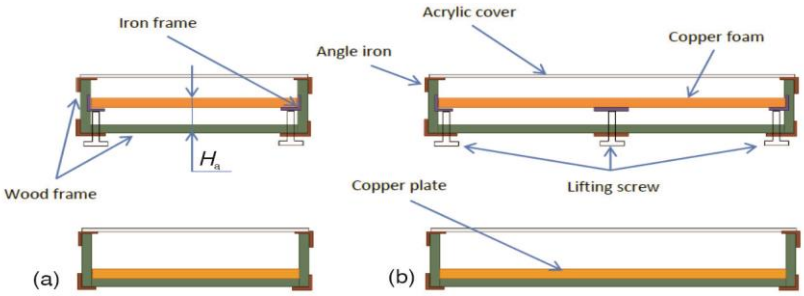

Figure 5. Location of copper foam in-channel of solar chimney; (a) front view and (b) side view

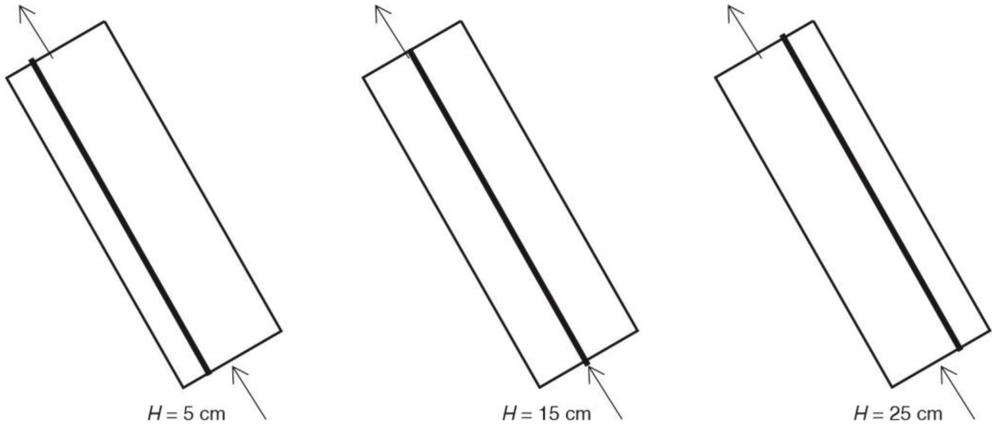

Figure 6. Position of metal foam in channel of solar chimney

Experimental test procedure

The test procedure for all modes is generally based on recording data from the reader or accumulating data in the data logger. Each mode's test day was divided into multiple duration times, each lasting 60 minutes. From May to July 2021, an experimental test was conducted in Baghdad (33.3° latitude, 44.4° longitude). The data is collected every one hour from 9:00 a. m. to 4:00 p. m. for clear days.

Many measurement and instrument devices are used in this study. The solar meter (TES-1333) is used to measure the incident solar radiation on the chimney's surface, and it is installed at an angle that works with the chimney. The accuracy of the solar power meter is within ±10 W/m^2 with spectral response 400-1100 nm and resolution of 0.1 W/m^2 for <1000 W/m^2 and 1 W/m^2 for ≥1000 W/m^2. The TES-132 interface data logger solar meter shown in fig. 7(a) is connected to the PC, to measure the solar intensity. The total solar radiation (includes beam and diffuse radiation) was measured on the surface of the chimney. A hot-wire anemometer probe model CEM-DT-8880, a sensor capable of measuring very low air velocities less than 0.5 m/s, is used to measure the air-flow velocity at the chimney's outlet. The

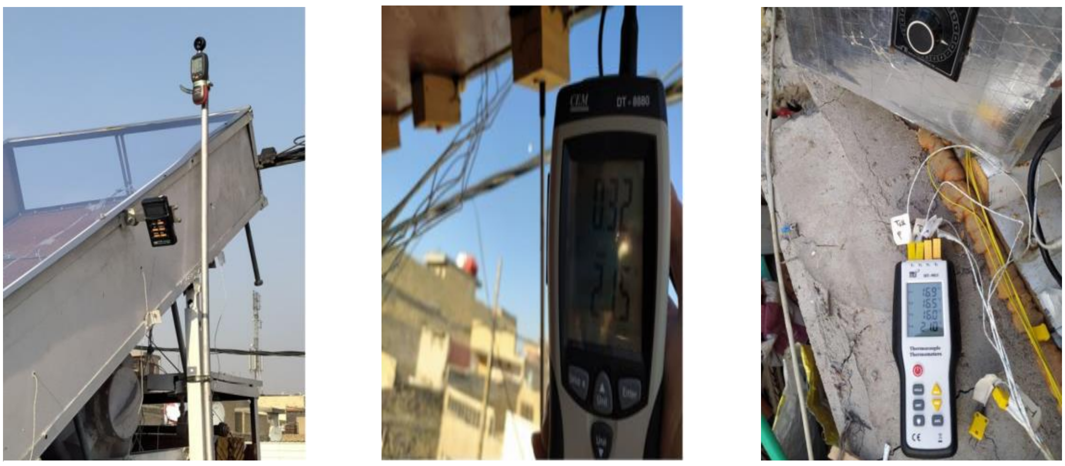

(a) (b) (c)

Figure 7. Measurements instruments used in experimental test; (a) solar meter and vane anemometer, (b) hot wire anemometer, and (c) thermocouples and data logger

accuracy of this instrument was stated to be ±1% of full scale, with a resolution of 0.01 m/s. By inserting this wire into the tilted solar chimney's gap, as shown in fig. 7(b). A hot wire anemometer is used to measure the average velocity at the outlet of the solar chimney. In this work, (63) thermocouples *k*-type has an accuracy of (±1.1 ºC) which were calibrated. Two temperature reading types (Thermo-Electric) and (Hi HT-9815) were used to connect the thermocouples for reading and saving data shown in fig. 7(c).

Eliciting data

It is essential to draw numerous conclusions from data elicitation, such as depicting the efficiencies of modes or assessing the performance of a mode's procedure, by comparing the data.

The solar chimney efficiency

To evaluate the solar chimney efficiency in ventilation and cooling modes with different solar chimney configurations and different inclination angles, by dividing the provided chimney useful energy by the total solar energy incident rate on its area at a specific time [25]:

$$\eta_c = \frac{Q_u}{Q_t} \tag{1}$$

The following formula is used to calculate the useful energy of the solar chimney:

$$Q_u = \dot{m}_{\text{air}} c_p \left(T_{\text{fo}} - T_{\text{fi}}\right) \tag{2}$$

The following formula can be used to calculate the amount of incident solar energy on the solar chimney area:

$$Q_i = I_t A_c \tag{3}$$

The area of the solar chimney can be obtained as:

$$A_c = (wL) \tag{4}$$

Air change per hour

The volume of air added to or removed from space in one hour is known as the rate of ACH. The air change per hour can be determined as the ratio of the volume flow rate to the total room volume. The total room volume is calculated using the ASHRAE stand of an actual room size of 27 m^3 [26]. The ventilation rate in real-life conditions is indicated by the air change found [27]:

$$ACH = \frac{V'}{V} \tag{5}$$

The volume flow rate can be obtained as:

$$V' = (A_o v_o 3600) \tag{6}$$

The volume of the test room can be determined as:

$$V = (L_r W_r H_r) \tag{7}$$

The properties of air were evaluated at air average temperature, which can be obtained as follow [28]:

$$T_\mathrm{f} = \varepsilon T_\mathrm{fo} + \left(1-\varepsilon\right) T_\mathrm{fi} \tag{8}$$

For the characteristics of air between 300 K and 350 K, the following relation is used [29, 30]:

$$c_p = \left[1.007 + 0.00004\left(T_\mathrm{f} - 300\right)\right]\cdot 10^3 \tag{9}$$

$$\rho_\mathrm{f} = \left[1.1614 - 0.00353\left(T_\mathrm{f} - 300\right)\right] \tag{10}$$

Error analysis

The accuracy of obtaining experimental results depends upon two factors. The accuracy of measurements and the design details of test rig. The deviations in accuracy are resulted from;
– The uniformities in heat flux on the wall surface.
– The alignment of fixing thermocouple.
– Errors in the accuracy of measuring devices.

There is no doubt, the maximum portion of errors in calculations referred essentially to the errors in the measured quantities. Hence, to calculate the error in the obtained results, the procedure of [31], is used in this field. Let the result, R, be a function of n independent variables (v_1, $v_2 \ldots v_n$):

$$R = R\left(v_1, v_2, \ldots, v_n\right) \tag{11}$$

For small variations in the variables, this relation can be expressed in linear form as:

$$\delta R = \frac{\partial R}{\partial v_1}\delta v_1 + \frac{\partial R}{\partial v_2}\delta v_2 + \ldots + \frac{\partial R}{\partial v_n}\delta v_n \tag{12}$$

Hence, the uncertainty intervals, w, in the result can be given as:

$$W_R = \left[\left(\frac{\partial R}{\partial v_1} w_1\right)^2 + \left(\frac{\partial R}{\partial v_2} w_2\right)^2 + \ldots + \left(\frac{\partial R}{\partial v_n} w_n\right)^2\right]^{0.5} \tag{13}$$

Equation (13) is greatly simplified to non-dimensional form as:

$$\frac{W_R}{R} = \left[\left(\frac{\partial R}{\partial v_1}\frac{w_1}{R}\right)^2 + \left(\frac{\partial R}{\partial v_2}\frac{w_2}{R}\right)^2 + \ldots + \left(\frac{\partial R}{\partial v_n}\frac{w_n}{R}\right)^2\right]^{0.5} \tag{14}$$

Hence, the experimental errors that may happen in the used variables are given in tab. 1 which is taken from measuring devices.

Table 1. Uncertainties of measuring tools

Independent variables, v	Uncertainty interval, w
Temperature	±0.1 ºC
Incident radiation	±10 W/m^2
Mass-flow rate	±0.001 kg/s

Results

The intensity of solar radiation was measured by data recorder solar power meter (TES-1333) for Baghdad, at latitude 33.3° N, longitude 44.4° E. Figures 8(a)-8(d) show the variation of measured the intensity of solar radiation (May-July 2021) with time on clear days from 09:00 a. m. to 04:00 p. m. for the test days on May, June, and July. The intensity of solar radiation increases steadily with time and reaches its peak value at the mid-day then decreases steadily towards sunset. The maximum solar radiation intensity reached to (986 W/m^2) at 12:00 noon on the 4th of July.

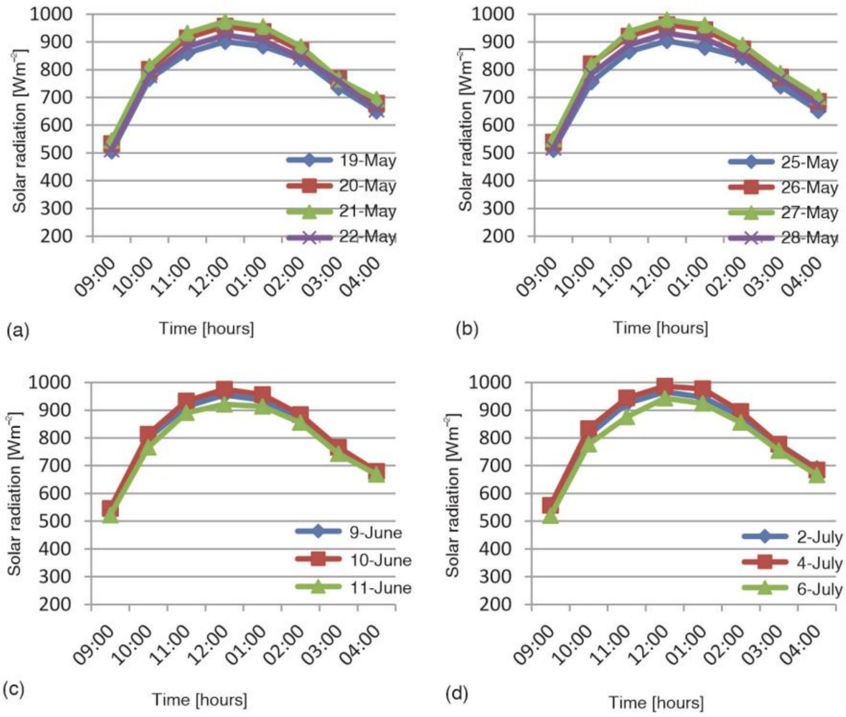

Figure 8. Variation of solar radiation values with time for different dates

Figure 9 shows the variation in ambient air temperature with time for the same dates as those shown in fig. 8. In addition, it can be noted that an increase in the intensity of solar radiation is associated with an increase in the temperature of the ambient air; however, a decrease in the temperature of the ambient air occurs later during the sunset period when compared to a decrease in the intensity of solar radiation after 12:00 p. m. This is due to the thermal energy stored in the buildings and surrounding regions during the sunrise, which is then released into the surrounding air during the sunset to heat the surrounding environment.

From May to July 2021, the tests were outdoors. The experiments were done between 9:00 a. m. and 4:00 p. m. on clear days. Figure 10 compares the variation of the mean absorber plate temperature over time for a 5 cm absorber plate height and a 60° inclination angle in May. Three absorber plates were used: flat plate, metal foam 10 PPI, and metal foam 40 PPI (May 19-28, 2021). The average absorber plate temperature (flat plate and metal foam

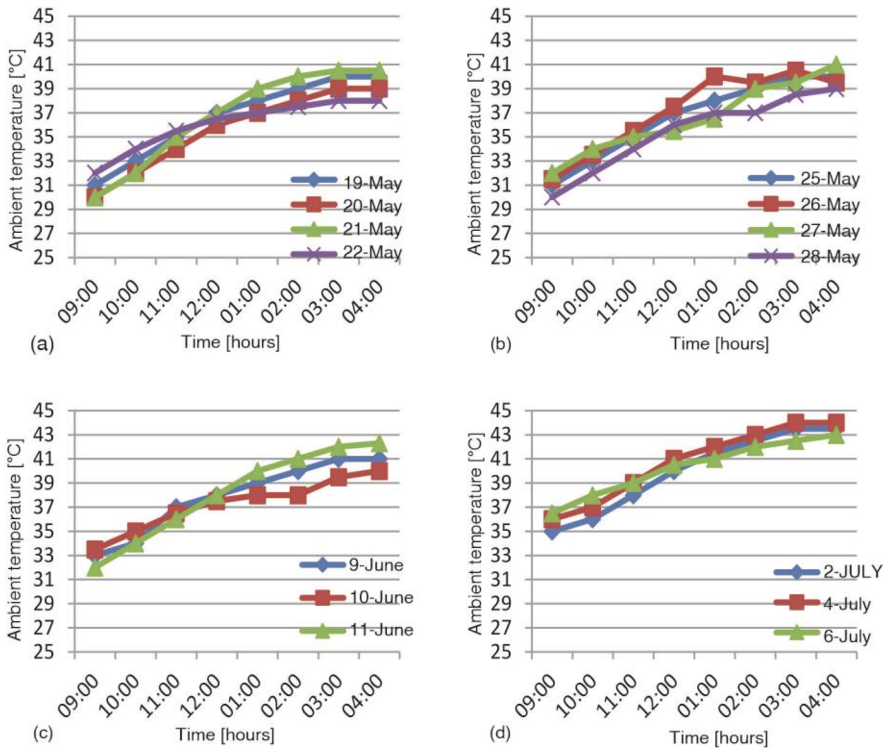

Figure 9. Variation of ambient temperature with time for different dates

10 PPI, 40 PPI) increases with increasing solar radiation intensity, but decreases with decreasing solar radiation intensity since 12:00 p. m. . After 12:00 p. m., the absorber plate remained warmer due to the stored thermal energy. During the same solar intensity in May, the maximum mean temperature difference between the (Flat plate and metal foam 10 PPI) absorber plate was 13.5°, and between the (flat plate and metal foam 40 PPI) absorber plate was 8.3°. Close inspection reveals that the metal foam absorber plate is cooler than the absorber plate without metal foam. Because air passes over, though, and lower the metal foam absorber plate, whereas air only passes upper and lower the absorber plate when there is no metal foam, the mean absorber plate temperature decreased (flat plate). Also, the flat absorber plate has a smaller surface area than the metal foam absorber plate, which increased the metal foam's air-flow. Figure 11 compares the temperature variation of three types of absorber plates: flat plate, metal foam 10 PPI, and metal foam 40 PPI, which used with different dates (May 19-28, 2021) for the same intensity of solar radiation. The absorber plate was 5 cm high and incline 60°. As shown in the figure, the absorber (metal foam) temperature rises gradually from the solar chimney inlet to the solar chimney end, peaking at the chimney's end, because of the thermal boundary-layer and the chimney absorber plate. The temperature increases along the absorber plate are not uniform, and the magnitude of the temperature increases significantly before the flat absorber plate ends. This is because the maximum boundary-layer thickness occurs before the flat absorber plate ends. When using metal foam, the maximum boundary-layer thickness is formed at the end of the chimney porous absorber plate due to the increased buoyancy effect caused by the increased surface area of the porous absorber plate. Figure 12 shows the mean absorber plate temperature variation over time for metal foam

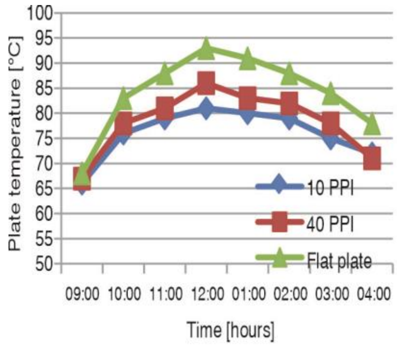

Figure 10. Average wall temperature for (flat, 10 PPI, and 40 PPI) absorber plate with time

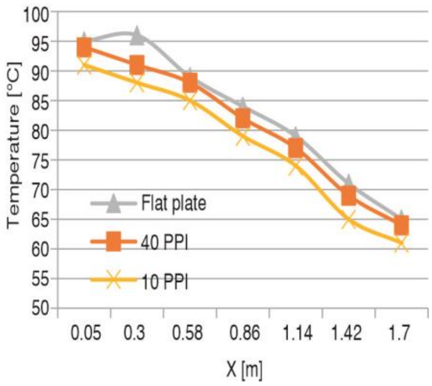

Figure 11. Absorber plate temperature for (flat plate, 10 PPI, and 40 PPI metal foam) with position

absorber plate (10 PPI) in June at 60° inclination. Three absorber plate heights (5 cm, 15 cm, and 25 cm) were used with three dates (Jun 09-11, 2021). The mean temperature of the absorber plate increases with height, reaching a maximum with H = 25 cm. In order to increase the flow through the metal foam, the absorber plate height was raised. However, the boundary-layer expanded over the metal foam, preventing heat exchange between the air and metal foam, causing an increase in absorber plate temperature.

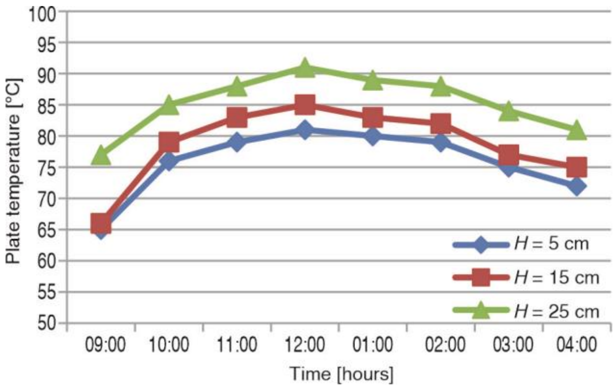

Figure 12. Average surface temperature for 10 PPI different absorber plate heights with time

Figure 13 shows a comparison between the variation of the average air temperature inside the chimney gap of the upper and lower with time at the same intensity of solar radiation in May and for absorber plate height of 5 cm and inclination angle 60°. Three types of absorber plate which flat plate, metal foam 10 PPI, and metal foam 40 PPI were used with different dates (May 19-28, 2021). The maximum mean air temperature of air-flow that logged between the (flat plate, metal foam 10 PPI, and metal foam 40 PPI) absorber plate was (78.5 °C) for 10 PPI at inclination angle 60° on the same solar intensity in May, while (75°C) for metal foam 40 PPI absorber plate and (64°C) for the flat plate at inclination angle 60° on the same solar intensity in May. It is concluded that a variation in the average air temperature with metal foam absorber plate shows that the growth of thermal boundary-layers is higher compared to a flat absorber plate, which indicates that the increases in air-flow induced by metal foam have contributed to this growth. Figures 14 show the mean air temperature variation with time for metal foam absorber plate (10 PPI) at the same intensity of solar radiation in June and for inclination angle 60°. Three different values of absorber plate heights (5 cm, 15 cm, and 25 cm) respectively were used with different dates (June 09-11, 2021). The maximum mean air temperature of air-flow that logged for the metal foam 10 PPI absorber plate was (78.5 °C) for the upper of the metal foam absorber plate at H = 5 cm while (70°C) for the lower of the metal foam absorber plate at H = 5 cm. It is clear that the mean temperature of air-flow increase with the decrease of absorber plate height due to the ability of heat exchange between the air and metal foam in this height and for the same reason mentioned previously.

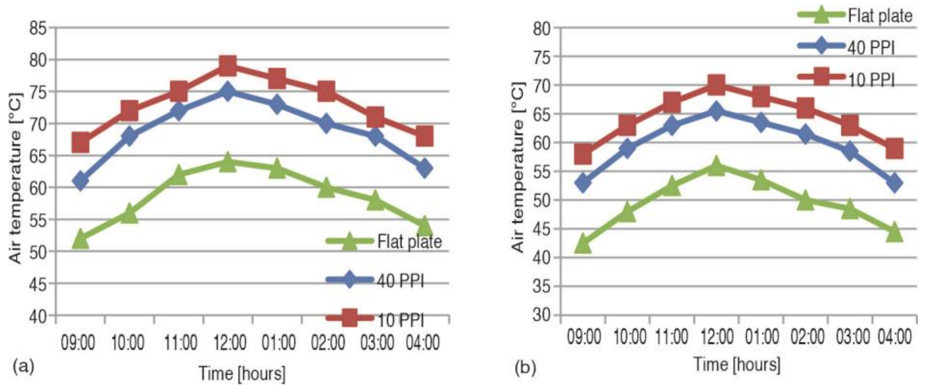

Figure 13. Average air temperature for; (a) upper and (b) lower of the (flat plate, 10 PPI, and 40 PPI) absorber plate with the time

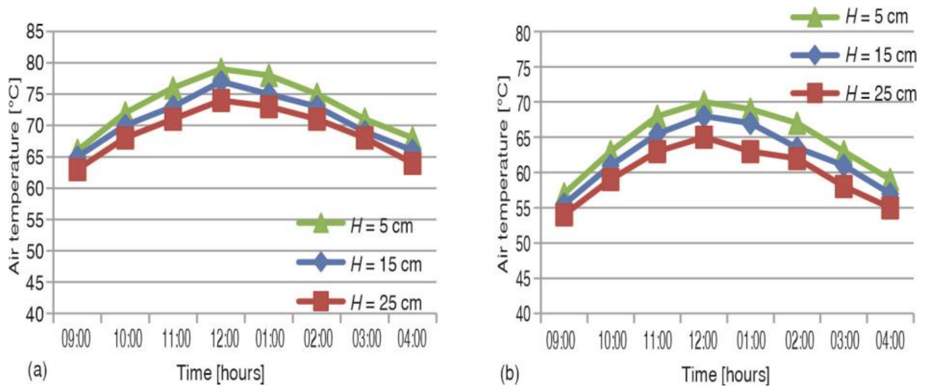

Figure 14. Average air temperature for; (a) upper and (b) lower of the 10 PPI absorber plate with time for different absorber plate heights

Figures 15 and 16 show the average room temperature inside the test room at the same intensity of solar radiation in all experimental tests during day hours (July 2021) in Baghdad. Three types of absorber plates of the solar chimney are a flat absorber plate, metal foam 10 PPI, and metal foam 40 PPI absorber plates for different angles and different absorber plate heights. Following the peak value of solar irradiance, the results show that the temperature difference between room temperature and outdoors increases by approximately 1.3 °C above ambient temperature. That results in an uncomfortable zone for humans, but it can be transformed into a pleasant air movement, especially during the last few days of March and the first few days of April. Alternatively, the ventilation effect can be used to remove undesirable gases and odors from rooms, auditoriums, and workshops at various times throughout the day and night. Figures 17 show a comparison between the variation of the average air velocity at the solar chimney with time at the same intensity of solar radiation in May and for absorber plate height of 5 cm and inclination angle 60°. Three types of absorber plate which flat plate, metal foam 10 PPI, and metal foam 40 PPI were used with different dates (May 19- 28, 2021). The maximum mean air-flow velocity that logged between the (flat plate, metal foam 10 PPI, and metal foam 40 PPI) absorber plate was (0.68 m/s) for 10 PPI at inclination angle 60° on the same solar intensity in May, while (0.61 m/s) for metal foam 40 PPI absorber plate and (0.47 m/s) for the flat plate at inclination angle 60° on the same solar intensity in May. As can be seen in the figures, the presence of the metal foam as an absorber plate resulted in a significant increase in air velocity when compared to when the absorber plate was flat. This is due to the presence of the metal foam absorber plate, which contains pores that increase the surface area, and this will have a positive impact on the quantity of heat transferred while also causing an increase in the air velocity towards the solar chimney exit, as shown in the figures.

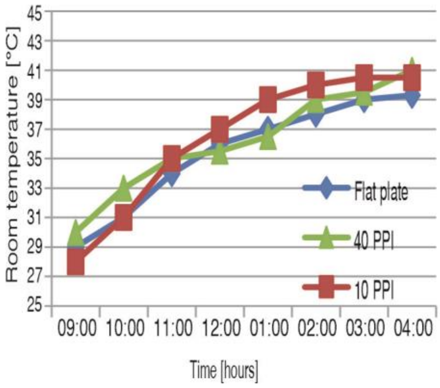

Figure 15. Average room temperature of (flat, 10 PPI, and 40 PPI) absorber plate with time

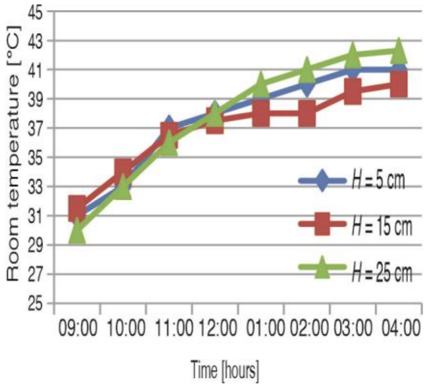

Figure 16. Average room temperature of 10 PPI with Time at different absorber plate heights

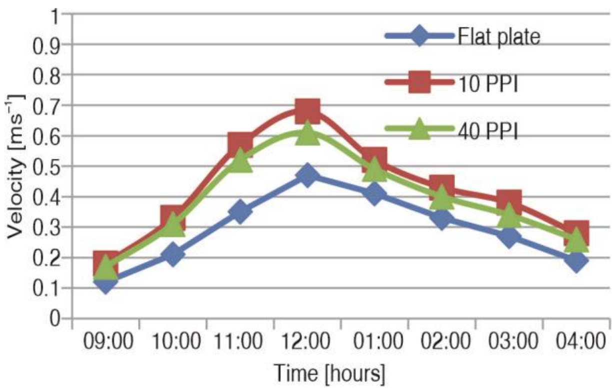

Figure 17. Variation of chimney velocity of (flat, 10 PPI, and 40 PPI) absorber plate with the time

Figures 18 show the average air velocity at the solar chimney with time for metal foam absorber plate (10 PPI) at the same intensity of solar radiation in June and for inclination angle 60°. Three different values of absorber plate heights (5 cm, 15 cm, and 25 cm) respectively were used with different dates (Jun 09-11, 2021). It is noted that the average air velocity of the solar chimney increase with the decrease of absorber plate height to reach the maximum value with H = 5cm. Due to the fact that when the absorber plate height was raised, the boundary-layer expanded over the metal foam, and therefore, the potential energy and buoyancy force can't be able to raise the flow-through metal foam so, don't occur heat exchange between the air and metal foam which in turn leads to decrease in air velocity of the solar chimney.

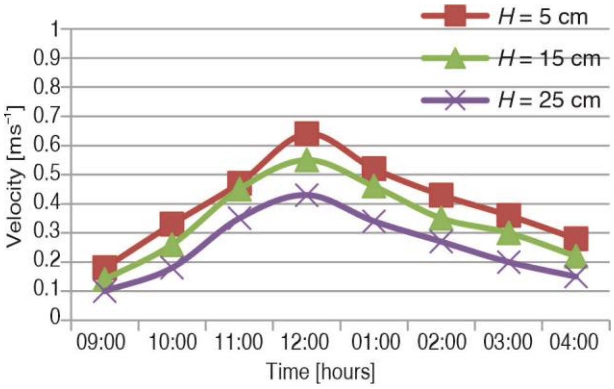

Figure 18. Variation of chimney velocity of 10 PPI of different absorber plate heights with time

Figures 19 show a comparison between the variation of the thermal efficiency of the solar chimney with time at the same intensity of solar radiation in May and for absorber plate height of 5 cm and inclination angle 60°. Three types of absorber plate which flat plate, metal foam 10 PPI, and metal foam 40 PPI were used with different dates (May 19-28, 2021). From these figures, as the intensity of the solar radiation increases, the general behavior of the thermal efficiency of the solar chimney (flat plate and metal foam 10 PPI and 40 PPI) increases. The maximum mean thermal efficiency of the solar chimney that logged between the (flat plate and metal foam 10 PPI) absorber plate was 49% and 72.1%, respectively, at inclination angle 60° on 21th of the same solar intensity in May, while between the (flat plate and metal foam 40 PPI) absorber plate was 49% and 66.2%, respectively, at inclination angle 60° on 27th of the same solar intensity in May. If you look at it closely, it is obvious that the thermal efficiency of the solar chimney of the metal foam absorber plate is higher than the thermal efficiency of the solar chimney of the flat plate absorber plate (without the metal foam). It is that due to the flat absorber plate has a small surface area when compared to the metal foam absorber plate, which increased the amount of air-flow produced by the metal foam. Figures 20 show the average thermal efficiency of solar chimney variation with time for metal foam absorber plate (10 PPI) at the same intensity of solar radiation in June and for inclination angle 60°. Three different values of absorber plate heights (5 cm, 15 cm, and 25 cm), respectively, were used with different dates (Jun 09-11, 2021). It is noted that the average thermal efficiency of solar chimney decrease with the increase of absorber plate height to reach the maximum value of 71% with H = 5 cm. Due to the fact that when the absorber plate height was raised, the boundary-layer expanded over the metal foam, and therefore, the potential energy and buoyancy force cannot be able to raise the flow-through metal foam so, don't occur heat exchange between the air and metal foam which in turn leads to decrease in thermal efficiency of solar chimney.

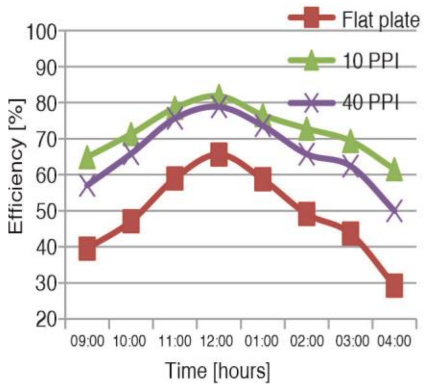

Figure 19. Chimney efficiency variation of (flat, 10 PPI, and 40 PPI) absorber plate time

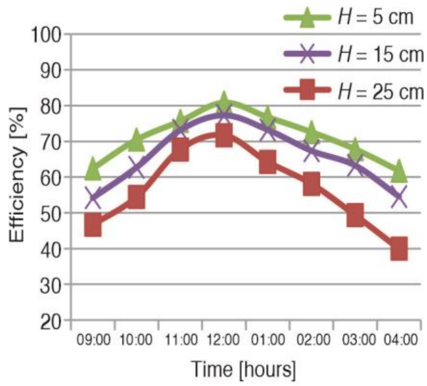

Figure 20. Chimney efficiency variation of 10 PPI at different absorber plate heights

Figures 21 show a comparison between the variation of the air change per hour in the test room with time at the same intensity of solar radiation in May and for absorber plate height of 5 cm and inclination angle 60°. Three types of absorber plate which flat plate, metal foam 10 PPI, and metal foam 40 PPI were used with different dates (May 19-28, 2021). From these figures, as the intensity of the solar radiation increases, the general behavior of the air change per hour in the test room (flat plate and metal foam 10 PPI and 40 PPI) increases. The maximum air change per hour in the test room that logged between the (flat plate and metal foam 10 PPI) absorber plate was (18.8 Lph) and (27.2 Lph), respectively, at inclination angle 60° on 21th of the same solar intensity in May, while between the (flat plate and metal foam 40 PPI) absorber plate was (18.8 Lph) and (24.4 Lph), respectively, at inclination angle 60° on 27th of the same solar intensity in May. If you look at it closely, it is obvious that the air change per hour in the test room for the metal foam absorber plate is higher than the air change per hour in the test room for the flat plate absorber plate (without the metal foam). It is that due the flat absorber plate has a small surface area when compared to the metal foam absorber plate, which increased the amount of air-flow produced by the metal foam. Figures 22 show the air change per hour in the test room variation with time for metal foam absorber

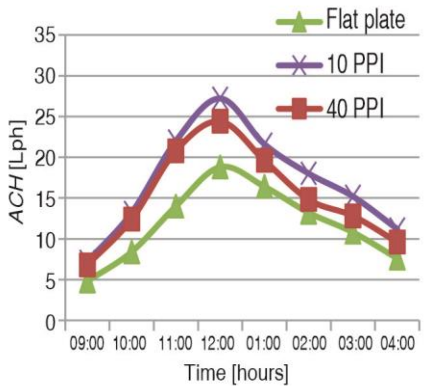

Figure 21. Air change per hour variation for (flat, 10 PPI, and 40 PPI) absorber plate with time

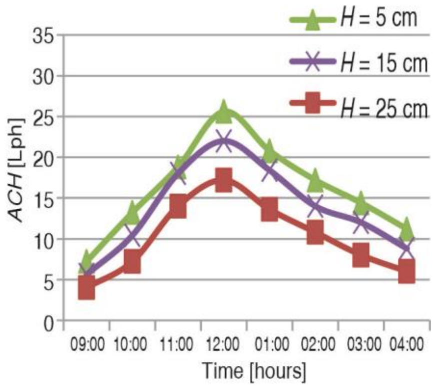

Figure 22. Air change per hour variation of 10 PPI different absorber plate heights with time

plate (10 PPI) at the same intensity of solar radiation in June and for inclination angle 60°. Three different values of absorber plate heights (5 cm, 15 cm, and 25 cm), respectively, were used with different dates (June 09-11, 2021). It is noted that the air change per hour in the test room decrease with the increase of absorber plate height to reach the maximum value (25.6 Lph) with H = 5 cm. Due to the fact that when the absorber plate height was raised, the boundary-layer expanded over the metal foam, and therefore, the potential energy and bouncy force cannot be able to raise the flow-through metal foam so, do not occur heat exchange between air and metal foam which in turn leads to decrease in air change per hour in the room.

Comparison with the previous experimental works

Experimental research is scant in the case of cooling mode in the test room with evaporative cooling and solar chimney using the metal foam as an absorber plate inside the solar chimney. Thus, in that respect, the results of the present experiments will be compared to other studies on the system's performance only with regard to the general behavior of some parameters. Figure 23 depicts the thermal efficiency of the solar chimney in a ventilated test room as a function of the heat flux (time). According to the findings of the current study, the general behavior of the thermal efficiency of solar chimney of a ventilated test room is similar to the experimental results obtained in the previous work. Take note in the figure that, as time passes, the heat flux increases, and the air change per hour of the ventilated test room increases, reaching its maximum possible value at 12:00 p. m. , when the heat flux is at its maximum, as discussed in previous sections as well. Observe in the figure that, as time progresses, the heat flux increases and the air change per hour of the ventilated test room increases, reaching its maximum possible value at 12:00 p. m., which corresponds to the time when the heat flux is at its maximum, and continuing to increase because the ambient temperature still increases, as previously discussed in the previous sections.

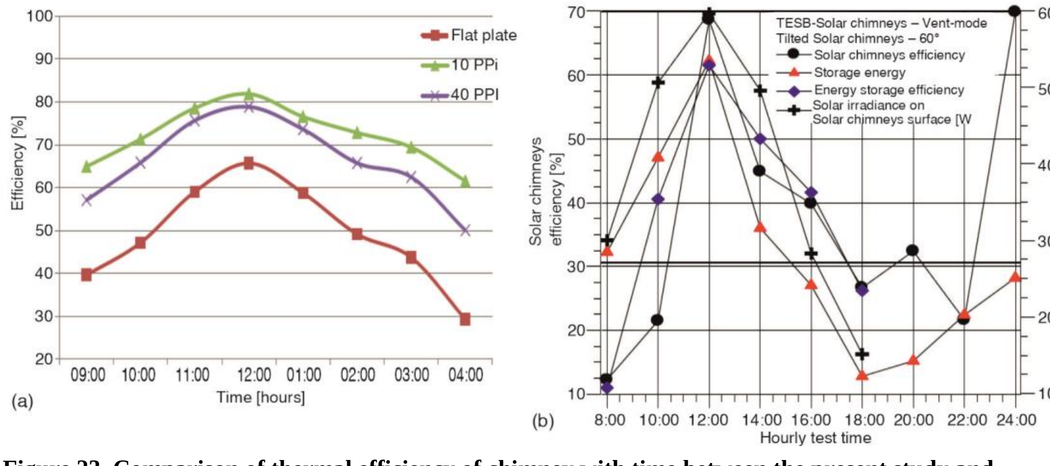

Figure 23. Comparison of thermal efficiency of chimney with time between the present study and the previous experimental result [32]; (a) present study and (b) [32]

Conclusions

Experimental studies have been carried out to investigate the improvement in heat transfer characteristics and overall performance of the solar chimney that was achieved by integrating with the test room and two-particle sizes (10 PPI and 40 PPI) metal foam absorber plates in the solar air chimney. On the natural convection heat transfer for different absorber plate heights of the metal foam absorber plate. During the months of May-July 2021, the experimental tests are carried out with three different types of chimney absorber plate (flat, 10 PPI, and 40 PPI) under Iraqi weather conditions and with five different heights of absorber plate. The following conclusions are drawn from the current investigation.

- Reducing the average temperature of absorber plate value. The highest reduction in the plate temperature was obtained experimentally with (10 PPI and 40 PPI) absorber plate (13.5 °C and 8.3 °C), respectively at θ = 60° compared to the conventional flat absorber plate.
- The maximum air-flow temperature with using (flat, 10 PPI, and 40 PPI) absorber plate is about (64 °C, 75 °C, and 78.5 °C), respectively, and increased with the increase of the absorber plate inclination angle from (30° to 75°).
- The maximum enhancement of the air-flow velocity at the solar chimney with (10 PPI and 40 PPI) absorber plate is recorded to about (27.3% and 11.1%), respectively, at θ = 45° and to about (43.7% and 25%), respectively, at θ = 60° compared to the conventional flat absorber plate.
- The air velocity at the solar chimney is decreased with the increase of the absorber plate heights. The percentage reduction in the air velocity from (5 cm to 25 cm) for 10 PPI absorber plate to about (48.8%), respectively.
- The thermal efficiency of the chimney is increased by using metal foam as an absorber plate (10 PPI and 40 PPI) to record maximum values at 12:00 p. m.. The maximum mean thermal efficiency of the solar chimney that logged between the (flat plate and metal foam 40 PPI, metal foam 10 PPI) absorber plate was 49%, 66.2%, and 72.1%, respectively, at an inclination angle of 60°.
- The maximum air change per hour in the test room that logged between the (flat plate and metal foam 40 PPI, metal foam 10 PPI) absorber plate was (18.8 Lph), (24.4 Lph), and (27.2 Lph), respectively, at inclination angle 60°.

References

[1] Yogesh, J., *Natural Convection, Heat and Mass Transfer*. Pergamon Press, Oxford, UK, 1980
[2] Smažilova, E., Papež, K., *Methods of Reducing Energy Consumption of Buildings Cooling System*, Czech Tech. Univer., Prague, Czech Republic, 2008
[3] Bansal, N. K., *et al*., A Study of Solar Chimney Assisted Wind Tower System for Natural Ventilation in Buildings, *Building and Environment, 29* (1994), 4, pp. 495-500
[4] Burek, S. A. M., Habeb, A., Air Flow and Thermal Efficiency Characteristics in Solar Chimneys and Trombe Walls, *Energy and Buildings, 39* (2007), 2, pp. 128-135
[5] Saifi, N., *et al*., Experimental Study and Simulation of Air-Flow in Solar Chimneys, *Energy Procedia, 18* (2012), Dec., pp. 1289-1298
[6] Di Cristofalo, S., *et al*., Thermal Behavior of «Scirocco Rooms» in Ancient Sicilian Villas, *Tunnelling and Underground Space Technology, 4* (1989), 4, pp. 471-473
[7] Sukhatme, S. P., *Solar Energy*, 4th ed., Tata McGraw Hill Pub. Company Limited, N. Y., USA, 1999
[8] Struckmann, F., Analysis of a Flat-Plate Solar Collector, Heat and Mass Transport, Project Report, Lund University, Lund, Sweden, 2008
[9] Bashair, A. H., Performance Evaluation of a Solar Chimney Provided with a Porous Absorber Plate; M. Sc. thesis, University of Baghdad, Baghadad, Iraq, 2019
[10] Ashby, M. F., Lu, T., Metal Foams: A Survey, *Science in China, Series B, 46* (2003), 6, pp. 521-532
[11] Shao, L., Riffat, S. B., Flow Loss Caused by Heat Pipes in Natural Ventilation Stacks, *Applied Thermal Engineering, 17* (1997), 4, pp. 393-399

[12] Khedari, J., *et al*., Ventilation Impact of a Solar Chimney on Indoor Temperature Fluctuation and Air Change in a School Building, *Energy and Buildings, 32* (2000), 1, pp. 89-93
[13] Raman, P., *et al*., A Passive Solar System for Thermal Comfort Conditioning of Buildings in Composite Climates, *Solar Energy, 70* (2001), 4, pp. 319-329
[14] Kotani, H., *et al*., "Development of Solar Chimney with Built-In Latent Heat Storage Material for Natural Ventilation, Department of Architectural Engineering, Osaka University, Accessed at the World Wide Web: http://serverlabo4. arch. eng. osaka-u. ac. Jp, 2005
[15] Barbara, L., Comparison between Numerical and Observed Air and Contaminant Distribution for Mechanical Mixing and Displacement Ventilation Coupled with a Local Exhaust-Lessons Learnt, *International Journal of Ventilation, 7* (2008), 3, pp. 233-250
[16] Leticia, N., *et al*., Modeling a Solar Chimney for Maximum Solar Irradiation and Maximum Air Flow, for Low Latitude Locations, *Proceedings of Building Simulation, 2011* (2011), pp. 14-16
[17] Amori, K. E., Saif W. M., Experimental and Numerical Studies of Solar Chimney for Natural Ventilation in Iraq, *Energy and Buildings, 47* (2012), Apr., pp. 450-457
[18] Naci, K., Daftekin, I., Passive Cooling Technology by Using Solar Chimney for Mild or Warm Climates, *Thermal Science, 20* (2016), 6, pp. 2125-2136
[19] Touma, A., *et al*., Solar Chimney Integrated with Passive Evaporative Cooler Applied on Glazing Surfaces, *Energy, 115* (2016), Part 1, pp. 169-179
[20] Zha, S., *et al*., Annual Energy Performance Simulation of Solar Chimney in a Cold Winter and Hot Summer Climate, *Building Simulation Tsinghua University Press, 12* (2019), 5, pp. 847-856
[21] Sujeeva, S., *et al*., Solar Chimney for a Real Building Considering Both Energy-Saving and Fire Safety– a Case Study, *Energy and Buildings, 221* (2020), 110016
[22] Shbailat, S. J., Nima, M. A., Possible Energy Saving of Evaporative Passive Cooling Using a Solar Chimney of Metal Foam Porous Absorber, *Energy Conversion and Management, X 12* (2021), 100118
[23] Ma, J., Liu, Y., Passive Solar Energy Building in Mountain Residence: Strategies and Design, *Thermal Science, 25* (2021), 3B, pp. 2263-2268
[24] Al-Saraf S. A. A. H., Performance Analysis of Solar Tower Integrated with Flat Plate and Copper Foam Absorber, Ph. D. thesis, University of Baghdad, Baghdad, Iraq, 2019
[25] Duffie, J. A., Beckman, W. A., *Solar Radiation*, Solar Engineering of Thermal Processes, 4th. ed., Hoboken, New Jersey, USA, 2013, pp. 12-20
[26] Li, Y., Liu, S., Experimental Study on Thermal Performance of a Solar Chimney Combined with PCM, *Applied Energy, 114* (2014), Feb., pp. 172-178
[27] Bassiouny, R., Korah, N. S. A., Effect of Solar Chimney Inclination Angle on Space Flow Pattern and Ventilation Rate, *Energy and Buildings, 41* (2009), 2, pp. 190-196
[28] Jalil, J. M., Khalaf, Z. J., Induced Buoyancy in Inclined Solar Chimney for Natural Ventilation, *Engineering and Technology Journal, 29* (2011), 2, pp. 183-194
[29] Awbi, H. B., *Ventilation of Buildings*, Routledge, London, UK, 2002
[30] Stylianos, A., The Process of Heat Transfer and Fluid Flow in CFD Problems, *American Journal of Science and Technology, 1* (2014), 1, pp. 36-49
[31] Kline, S. J., Describing Uncertainty in Single Sample Experiments, *Mech. Eng., 75* (1953), pp. 3-8
[32] Murtadha, T. K., *et al*., Experimental Study Using Cooling With PCM and CFM, *Al-Khwarizmi Engineering Journal, 12* (2016), 3, pp. 80-98

Paper submitted: October 8, 2021
Paper revised: April 21, 2022
Paper accepted: May 4, 2022